

## Angular and radial temperature profiles in the thermal decomposition of wood

Rafael Bilbao, María Benita Murillo and Angela Millera

*Department of Chemical and Environmental Engineering, Faculty of Science,  
University of Zaragoza, 50009-Zaragoza (Spain)*

(Received 22 January 1992)

### Abstract

During the thermal decomposition of wood, an increase in the particle size produces an important decrease in the weight loss of the solid caused by significant temperature profiles, both radial and angular, inside the solid. In order to determine these profiles, experiments with different particle sizes (2, 3, 4 and 5.6 cm in diameter) have been carried out. In these experiments, temperatures at different points corresponding to various values of radii and angles were measured. An analysis of the different values and trends obtained has been performed.

### INTRODUCTION

In previous papers [1–5], several studies concerning the thermal decomposition of different lignocellulosic materials carried out in a thermobalance in a nitrogen environment have been published. Using small particle sizes, the behaviour of cellulose [1,2], xylan and lignin [3], and “Pinaster” pine and barley straw [4,5] was analysed.

In the case of the reactors used in gasification and pyrolysis processes (moving bed, rotatory furnace etc.), larger particle sizes are used, and temperature profiles may be produced inside the solid. These profiles must be taken into account in the modelling of the thermal decomposition process, because of their influence on the solid conversion and on the product distribution obtained in the pyrolysis of lignocellulosic materials. This modelling must involve the resolution of the heat and mass balance equations, including the kinetic equations, the heat generated or consumed during the process and the heat transfer phenomena.

An experimental system was built that allows the use of large particle sizes and the simulation of different operating conditions [6,7]. This system

---

*Correspondence to:* R. Bilbao, Department of Chemical and Environmental Engineering, Faculty of Science, University of Zaragoza, 50009-Zaragoza, Spain.

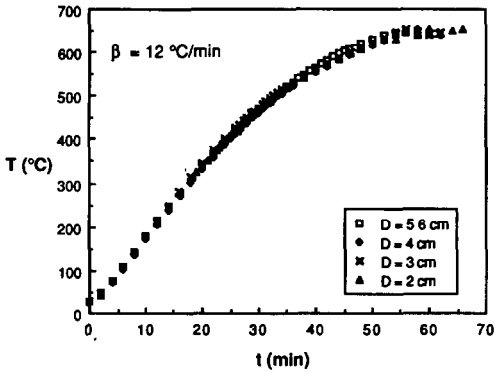


Fig. 1. System temperature versus time for different particle sizes.

enabled us to obtain the temperature profiles inside and outside the particle, and the weight loss of the solid during its thermal decomposition.

In a previous study [7], the temperature profiles inside the empty reactor, and the influence of the operating conditions on them, were studied in order to achieve the most homogeneous thermal environment around the particles.

This work presents the experimental results of the weight loss and temperature profiles in the thermal decomposition of different particle sizes of wood.

## EXPERIMENTAL METHOD

Using the system mentioned above, experiments were conducted from 30 to 650°C using a heating rate of 12°C min<sup>-1</sup>. Once 650°C was reached, the system remained at this temperature for 12 min.

Figure 1 shows the system temperature variation with time for the different experiments carried out.

Nitrogen was used as the inert gas, with a flow rate of 15 cm<sup>3</sup> s<sup>-1</sup>. The wood particle was placed in the reactor at a depth of between 12 and 18 cm. Previous studies [7] have indicated that these values are the most suitable operating conditions. Spherical pine wood particles with  $D = 2, 3, 4$  and 5.6 cm were used.

Two types of experiment were performed.

(i) Experiments were performed to obtain the temperature profiles inside the solid and on its surface. Thermocouples were placed at several points in the solid, corresponding to different values of  $\alpha$  ( $\alpha$  being the angle which sweeps the plane of the inert gas flow direction,  $\alpha = 0^\circ$  corresponding to the direction of the radius vector opposite to the flow direction and  $\alpha = 180^\circ$  with the flow direction) and  $r/R$  (reduced radius).

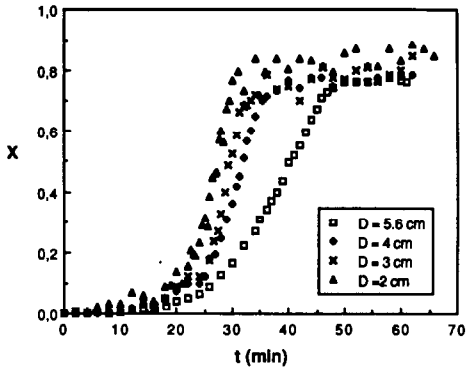


Fig. 2. Comparison of the values of solid conversion  $X$  obtained for different particle sizes.

The temperature was measured at different points corresponding to  $\alpha = 0, 45, 90, 135$  and  $180^\circ$  and  $r/R = 0, 0.47, 0.83$  and  $1.0$ .

(ii) Experiments were performed to obtain the weight loss of the solid versus time.

## RESULTS AND DISCUSSION

The results obtained for the weight loss versus time for the different particle sizes are shown in Fig. 2. It is observed that as the particle size increases, so does the time required to obtain a determinate conversion. This effect is very noticeable when a particle 5.6 cm in diameter is used.

When the system temperatures in the four cases are compared, it can be seen that these are very similar (see Fig. 1). Therefore the different conversions obtained at the same time for the different particle sizes may be due to the different temperatures in the solid.

In a previous paper [7], it was shown that the temperature on the solid surface varies, depending on the value of  $\alpha$ , and this variation was different for the different particle sizes. This was due to the fact that the points on the solid surface correspond to distinct radii in the reactor which have different temperatures.

Furthermore, for a certain solid size, appreciable angular and radial temperature profiles appear in the particle itself.

Figure 3 shows the solid surface temperatures at several values of  $\alpha$ , obtained in a particle of  $D = 5.6$  cm. In the range of  $0^\circ \leq \alpha \leq 90^\circ$ , the temperature increases with  $\alpha$ , which can be explained by the different reactor radii that correspond to the different points on the solid surface and by the influence of the deviation in the gas flow direction [7]. For values of  $\alpha$  from  $90^\circ$  to  $180^\circ$ , both effects are compensated by each other, and the temperatures obtained at distinct values of  $\alpha$  are very similar.

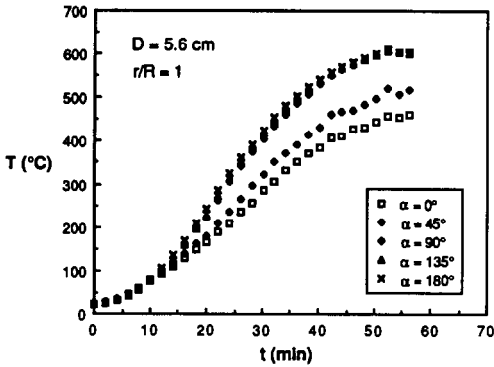


Fig. 3. Angular temperature profiles on the solid at  $r/R = 1$  and  $D = 5.6$  cm.

Angular temperature profiles also appear inside the solid. The results obtained at  $r/R = 0.47$  are shown in Fig. 4. Again, the temperature increases with  $\alpha$  in the range  $0^\circ \leq \alpha \leq 90^\circ$ , and for values of  $\alpha \geq 90^\circ$  the temperatures are similar. It must be noted that these angular temperature profiles are less noticeable than those observed on the solid surface.

Similar trends are noticed with the other particle sizes. Figures 5 and 6 show the temperatures measured on the solid surfaces of particles 4 and 3 cm in diameter. It may be noted that the variation of temperature with  $\alpha$  is smaller as the particle size diminishes, which may be due to the fact that as the solid size decreases the reactor radii corresponding to the different values of  $\alpha$  are more similar, and the deviation in the gas flow direction is less important. Therefore, as can be seen in Figs. 7 and 8, the smaller the particle, the smaller the angular temperature profiles inside the solid.

These angular temperature profiles on the solid surface, together with the conduction and convection heat transfer mechanisms and the heat generated and/or consumed during the thermal decomposition of the

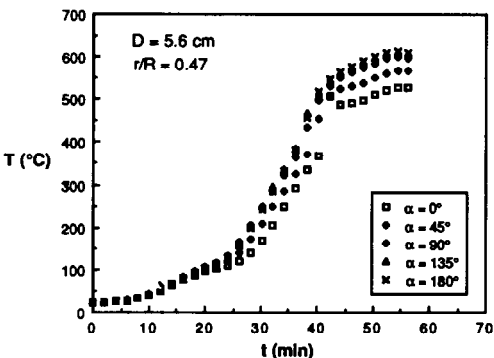


Fig. 4. Angular temperature profiles in the solid at  $r/R = 0.47$  and  $D = 5.6$  cm.

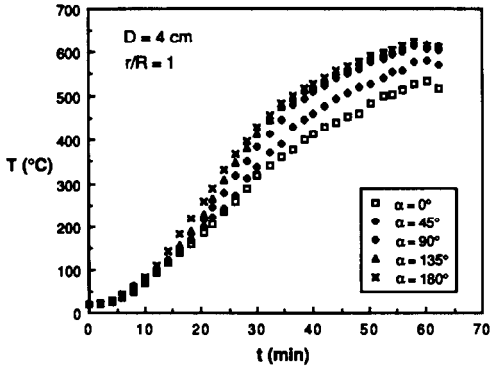


Fig. 5. Angular temperature profiles on the solid at  $r/R = 1$  and  $D = 4$  cm.

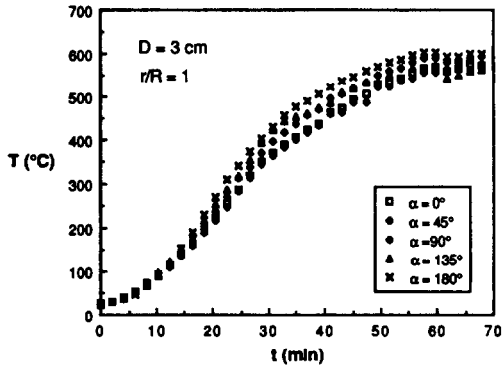


Fig. 6. Angular temperature profiles on the solid at  $r/R = 1$  and  $D = 3$  cm.

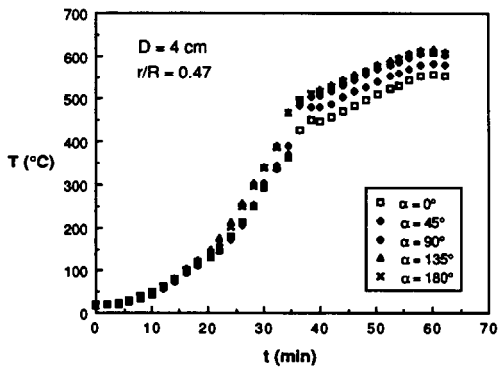


Fig. 7. Angular temperature profiles in the solid at  $r/R = 0.47$  and  $D = 4$  cm.

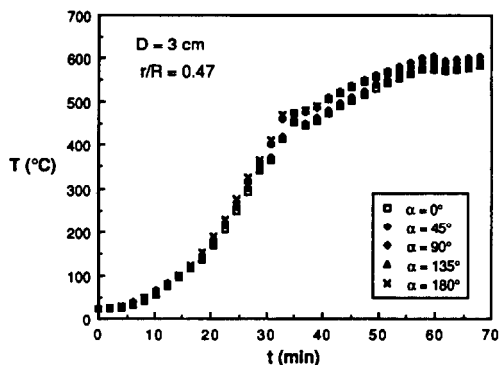


Fig. 8. Angular temperature profiles in the solid at  $r/R = 0.47$  and  $D = 3$  cm.

material, result in important radial temperature profiles appearing in the solid, which depend on the value of  $\alpha$ .

Figures 9–11 show the radial temperature profiles obtained in a particle 5.6 cm in diameter at three values of  $\alpha$ . These profiles are such that the temperature decreases as the radius decreases.

It is important to note that at the inner points, especially at  $r/R = 0$ , a plateau appears at 100°C in the temperature profile, the temperature remaining at this value for a certain time. During this time, the solid conversion is still low, therefore the influence of the heat of reaction is insignificant. Likewise, the predominant heat transfer mechanism inside the solid would be conduction and this cannot explain the plateau and the steep radial temperature profile existing at this time. For this reason, this period may correspond to the evaporation of moisture, which requires a determinate amount of the heat flow to be directed towards the interior of the solid.

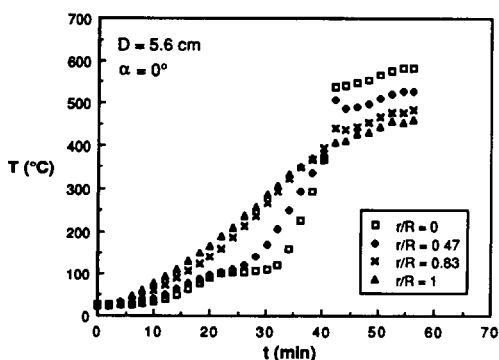


Fig. 9. Radial temperature profiles in the solid at  $\alpha = 0^\circ$  and  $D = 5.6$  cm.

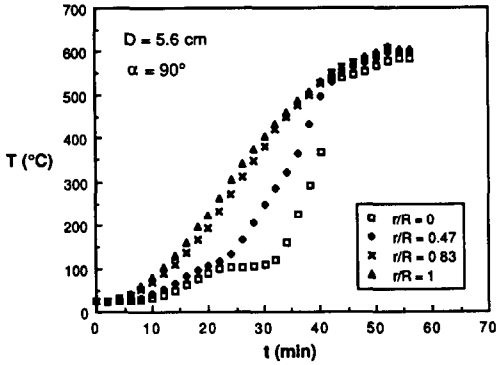


Fig. 10. Radial temperature profiles in the solid at  $\alpha = 90^\circ$  and  $D = 5.6$  cm.

At the end of the plateau, there is a sudden increase in the temperature at the inner points. This may be due not only to the conduction heat transfer caused by the high temperature differences (about 250–300°C) in the solid, but also to the hot gas flow from the exterior to the interior of the particle. While the inner point,  $r/R = 0$ , remains at 100°C, the other outer points achieve high temperatures so that their conversions are also high; in addition, the porosity becomes greater and therefore the hot gas flows easily into the solid, contributing to its increase in temperature.

In the three figures, a sharp increase in the slope of the temperature versus time curve is also observed near the end of the heating, being especially noticeable at  $r/R = 0$  and less steep at  $r/R = 0.47$ . This is probably due to the exothermic decomposition of the lignin [3], which prevails at high conversions.

For  $\alpha < 90^\circ$  and long reaction times an inversion in the radial temperature profiles is observed now that the temperature is higher as the value of  $r/R$  decreases. It is important to notice that this happens when the

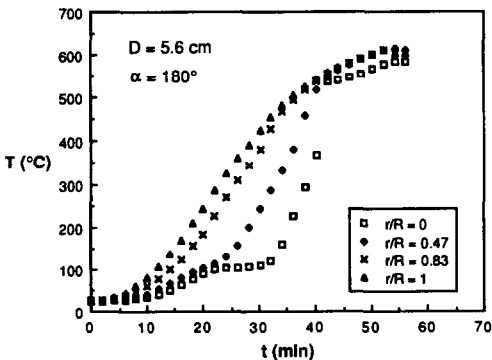


Fig. 11. Radial temperature profiles in the solid at  $\alpha = 180^\circ$  and  $D = 5.6$  cm.

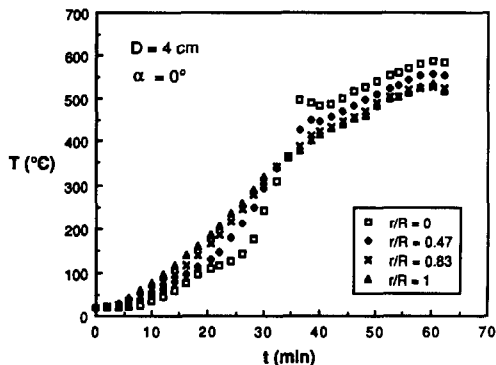


Fig. 12. Radial temperature profiles in the solid at  $\alpha = 0^\circ$  and  $D = 4$  cm.

conversion is total in the outer zones and high in the inner. This inversion may be explained mainly by the heat transfer mechanisms, because it is considered that the points with high values of  $\alpha$  have higher temperatures and this contributes to the rise in temperature at the inner points. The exothermic heat generated during the lignin thermal decomposition also contributes to this effect, because this exothermic process occurs at the inner points when the outer have already been converted.

As can be observed in Figs. 10 and 11, for  $\alpha \geq 90^\circ$  the inversion does not happen but an important reduction in the radial temperature profiles is produced.

The results obtained with a solid of  $D = 4$  cm are shown in Figs. 12–14. The same trends as in the previous case are observed, although they are less pronounced. For  $\alpha = 0^\circ$  (Fig. 12) an inversion in the radial temperature profiles is also noted, but in this case it is less steep, because the angular temperature profiles are smaller. Moreover, this inversion happens at shorter reaction times than in the case of  $D = 5.6$  cm. However, it is

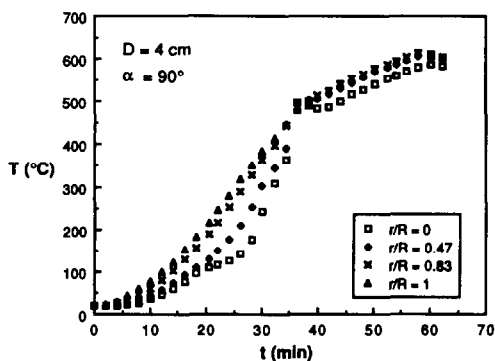


Fig. 13. Radial temperature profiles in the solid at  $\alpha = 90^\circ$  and  $D = 4$  cm.



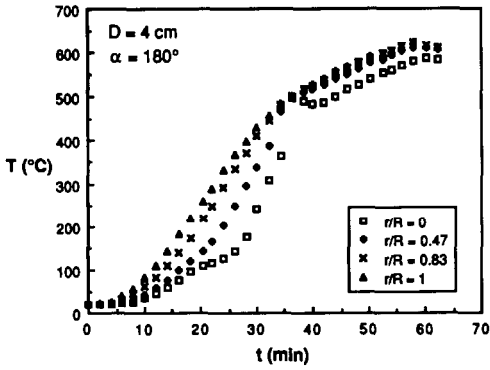


Fig. 14. Radial temperature profiles in the solid at  $\alpha = 180^\circ$  and  $D = 4$  cm.

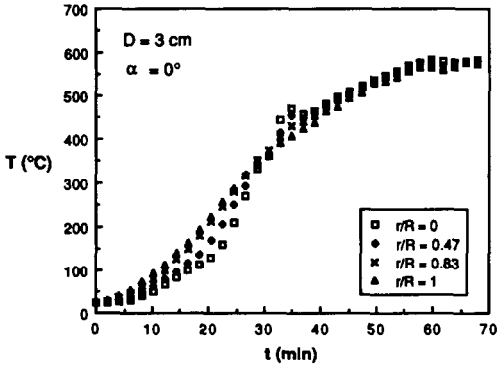


Fig. 15. Radial temperature profiles in the solid at  $\alpha = 0^\circ$  and  $D = 3$  cm.

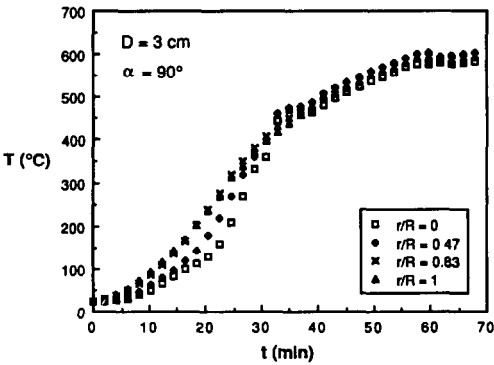


Fig. 16. Radial temperature profiles in the solid at  $\alpha = 90^\circ$  and  $D = 3$  cm.

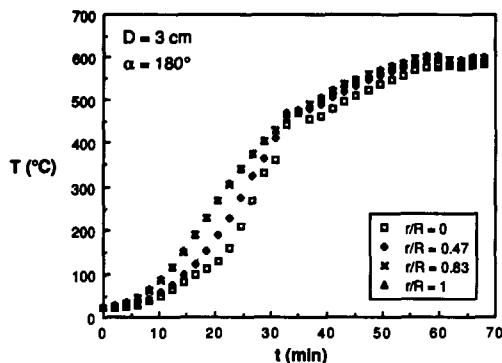


Fig. 17. Radial temperature profiles in the solid at  $\alpha = 180^\circ$  and  $D = 3$  cm.

interesting to note that in both cases,  $D = 5.6$  and  $4$  cm, the inversion occurs at very similar conversions (see Fig. 2) which strengthens the previous assumptions.

All the trends explained above can be also observed in the results obtained with particles  $3$  cm in diameter (Figs. 15–17). In this case, both radial and angular profiles are less marked, and in general all the trends observed for greater sizes are now much less noticeable. A slight inversion is also produced at  $\alpha = 0^\circ$  and at shorter reaction times than in previous cases.

The results corresponding to the particle size of  $D = 2$  cm have been shown in previous studies [6,7]. For this particle size, the radial and angular profiles are insignificant in comparison with the other particle sizes that have now been studied.

## CONCLUSIONS

(1) The different temperatures on the solid surface, together with the conduction and convection heat transfer mechanisms and the generated and/or consumed heat during the process, result in important angular and radial profiles appearing inside the solid. These profiles cause a more significant decrease in the solid conversion as the particle size increases.

(2) At  $100^\circ\text{C}$ , a delay in the temperature rise is produced at the inner points, especially when the particle size is large, probably due to the heat consumed by water evaporation.

(3) Just after the plateau ends, a sudden increase in the temperature occurs, caused mainly by the conduction and convection mechanisms.

(4) In the range  $\alpha \leq 90^\circ$ , an inversion in the radial temperature profiles is observed at long reaction times.

(5) All these trends become less important as the particle size decreases, being practically insignificant for  $D = 2$  cm.

#### ACKNOWLEDGEMENTS

The authors express their gratitude to D.G.I.C.Y.T. for providing financial support for this work (Project PB-88-0388) and also to Ministerio de Educación y Ciencia, Spain, for a research grant awarded to M.B. Murillo.

#### REFERENCES

- 1 R. Bilbao, J. Arauzo and A. Millera, *Thermochim. Acta*, 120 (1987) 121.
- 2 R. Bilbao, J. Arauzo and A. Millera, *Thermochim. Acta*, 120 (1987) 133.
- 3 R. Bilbao, A. Millera and J. Arauzo, *Thermochim. Acta*, 143 (1989) 137.
- 4 R. Bilbao, A. Millera and J. Arauzo, *Thermochim. Acta*, 143 (1989) 149.
- 5 R. Bilbao, A. Millera and J. Arauzo, *Thermochim. Acta*, 165 (1990) 103.
- 6 R. Bilbao, M.B. Murillo, A. Millera and J.F. Mastral, *Thermochim. Acta*, 190 (1991) 163.
- 7 R. Bilbao, M.B. Murillo, A. Millera, J. Arauzo and J.M. Caleyá, *Thermochim. Acta*, 197 (1992) 431.